Received: 30 May 2025 | Revised: 26 June 2025 | Accepted: 16 July 2025

DOI: 10.1111/ijac.70034

SPECIAL ISSUE ARTICLE

# UV curing of polysilazane-based coatings with metallic fillers for corrosion protection applications

**Jan-Felix Wendel**[1] | **Annika Fischer**[1] | **Daniel Leykam**[2] | **Stefan Schafföner**[1,3,4] | **Günter Motz**[1]

[1]Chair of Ceramic Materials Engineering, University of Bayreuth, Bayreuth, Bavaria, Germany

[2]Chair of Electrochemical Process Engineering, University of Bayreuth, Bayreuth, Bavaria, Germany

[3]Bayreuth Center for Materials Science and Engineering, University of Bayreuth, Bayreuth, Bavaria, Germany

[4]Bavarian Polymer Institute, Bayreuth, Bavaria, Germany

**Correspondence**
Günter Motz, Chair of Ceramic Materials Engineering, University of Bayreuth, Bayreuth, Bavaria 95447, Germany.
Email: guenter.motz@uni-bayreuth.de

**Abstract**

In this study, UV curing of polysilazane-based coating systems highly filled with metallic fillers for corrosion protection applications was examined. The UV curing was carried out using the thiol-ene "click" reaction. Therefore, a tetra-functional thiol crosslinking agent and a photoinitiator were added to the polysilazane to accomplish the radical crosslinking reaction. The UV-cured coating systems were compared to thermally cured samples regarding mechanical properties and chemical resistance. The mechanical properties were studied by scratch tests and hardness measurements and the chemical resistance by immersion in toluene and isopropanol. Contact angle measurements were carried out before and after the chemical resistance tests. Surprisingly, it was found that despite the high amount of metallic particles, the entire filled coating was cured by UV irradiation. The mechanical properties of the UV-cured systems were slightly worse compared to the thermally cured coatings. However, both curing methods led to a very good chemical resistivity of the coatings against the liquid polar and nonpolar media. Contact angle measurements revealed that by UV curing more hydrophobic coatings are achieved due to prevention of oxidation of the metallic fillers. Hence, UV curing is a suitable technique to crosslink also filled coatings offering interesting properties for corrosion protection applications.

**KEYWORDS**

lamellar coating, metallic filler, polysilazane-based coating, thiol-ene click reaction, UV curing

## 1 | INTRODUCTION

Due to the large economic damage caused by corrosion,[1] there is large variety of approaches to protect steel from corrosion. In salt water environments, zinc-based coatings are usually used due to their favorable properties. Zinc has a lower electrochemical potential compared to iron, and is therefore sacrificed while protecting the steel substrate. A subgroup of available zinc coatings are zinc-rich coatings, which contain spherical or lamellar zinc particles embedded in an organic or inorganic matrix.[2,3] These zinc-rich coatings effectively protect steel and offer some advantages including an easy application process by spraying or dipping and the absence of a possible hydrogen

embrittlement of the steel substrate, which can occur in the common hot-dip galvanizing process.[4,5] To function properly, the zinc particles need to be in an electrically conductive contact with each other and with the substrate. To ensure this contact and to increase the contact area between the particles, the usage of lamellar shaped pigments is a meaningful option.[6,7] Common matrix materials of zinc-rich coatings are epoxy resins,[8–10] silicates,[11–13] and titanates.[2] An alternative is the application of silazanes. Silazanes are preceramic polymers, which offer excellent properties that predestine them for the use in corrosion protection coatings. They possess a high chemical stability in corrosive environments and an excellent adhesion to metal surfaces because of the formation of covalent bonds to the substrate.[14,15] Coatings based on silazanes can be applied by easy application methods like spraying or dipping and are adjusted in their properties in a wide range using active or passive fillers.[16,17]

Polysilazane coatings are usually cured by a thermal treatment up to 500°C conducted in a furnace. This process is subjected to some limitations.[17] On the one hand, the properties of thermally sensitive substrates or filler materials can be impaired by the thermal treatment or they are not able to withstand the required temperatures leading to degradation. On the other hand, an economically viable thermal treatment of large components in a furnace is not always possible. Hence, alternative curing methods to crosslink silazane-based coatings are needed. UV curing was identified as an interesting and promising option. Several authors demonstrated the feasibility of curing preceramic polymers by UV irradiation.[18–20] A popular application of this technique is additive manufacturing,[18,21–30] but it was also used in freeze-casting[31,32] and for the fabrication of micro-electromechanical systems (MEMS),[33] for example. The rapid reaction kinetics allow the fabrication of complex structures and shapes, which makes UV curing attractive for these applications. A brief overview of the activities on UV curing of silicon-based coatings can be found in the review of Barroso et al.[17]

In a recent work of Hoffmann et al.,[34] polysilazane coatings were crosslinked by UV curing using a thiol-ene "click" reaction. For that purpose, a crosslinking agent was added to the polysilazane. The crosslinking agent possesses thiol groups, which form radicals activated by a UV-triggered photoinitiator leading to a radical crosslinking reaction with vinyl groups of the polysilazane.[20,23,31,32] The reaction includes chain propagation, chain transfer and chain growth reactions.[20,32,35]

To the best of the authors' knowledge, only precursor systems with at most a small amount of fillers or additives were used for UV curing. By transferring this technique to coating systems for corrosion protection applications, a much higher amount of metallic fillers has to be considered. Metallic fillers such as aluminum are not transparent but might reflect UV radiation, which complicates the curing of a highly filled coating system. If the UV radiation is reflected, curing may not occur sufficiently in the whole volume of the coating, which could then lead to a loss of cohesion or an impairment of the chemical and physical coating properties. Hence, the aim of this work is to evaluate the feasibility of UV curing for polysilazane-based coating systems filled to 80 vol.% with metallic fillers. For this purpose, thermally and UV-cured coatings were investigated. Both corrosion protection coating systems were thoroughly analyzed and compared regarding their microstructure, hardness, scratch resistance, and chemical resistance to various media. Moreover, to understand the UV curing mechanisms, UV-Vis measurements were conducted.

## 2 | MATERIALS AND METHODS

The compositions of the used steel substrates are given in Tables 1 and 2. Sheets of steel 1.7335 (13CrMo4-5, HSM Stahl- und Metallhandel GmbH, Germany) with a thickness of 2 mm was used for the characterization of the coatings' mechanical properties and microstructure due to the wide industrial engineering application of this steel grade. On the other hand, the steel grade 1.4310 (X10CrNi18-8, HSM Stahl- und Metallhandel GmbH, Germany) with a thickness of 0.2 mm was chosen for chemical resistance tests due to its chemical inertness resulting from a high degree of alloying and its availability as thin sheets. Both materials were cut in dimensions of 70 mm × 30 mm. To remove the oxide layer, the 1.7335 steel samples were additionally sandblasted. Afterward all samples were cleaned in an ultrasonic bath in acetone for 20 min and then dried.

The commercially available precursor Durazane 1800 (Figure 1A, Merck KGaA, Germany) from the group of organosilazanes was applied as the matrix material for the coating systems. Crosslinking of the functional groups was conducted in two different ways. For thermal curing, 3 wt.% of the radical initiator dicumyl peroxide (DCP, Sigma Aldrich GmbH, Germany) was added to the Durazane 1800. DCP acts as an initiator for the crosslinking reaction and reduces its initial temperature and the volatilization of oligomers.[36] Durazane 1800 without DCP was used for UV crosslinking. Instead, pentaerythritol tetrakis(3-mercaptopropionate) (TT, Figure 1B, Sigma Aldrich GmbH, Germany) was selected as the reactant for the thiol-ene "click" reaction. TT was added in different molar ratios (mol thiol groups of TT relative to mol vinyl groups of Durazane 1800) corresponding to 10%, 50%, and 100% of reacted vinyl groups provided by the precursor. The different TT contents were chosen in order to

**TABLE 1** Composition of the steel 1.7335.

| Element | C | Si | Mn | P | S | N | Cu | Cr | Mo | Fe |
|---|---|---|---|---|---|---|---|---|---|---|
| **Min (wt.%)** | 0.08 | – | 0.40 | – | – | – | – | 0.70 | 0.40 | Bal. |
| **Max (wt.%)** | 0.18 | 0.35 | 1.00 | 0.025 | 0.010 | 0.012 | 0.30 | 1.15 | 0.60 | Bal. |

**TABLE 2** Composition of the steel 1.4310.

| Element | C | Si | Mn | P | S | Cr | Mo | N | Ni | Fe |
|---|---|---|---|---|---|---|---|---|---|---|
| **Min (wt.%)** | 0.05 | – | – | – | – | 16.00 | – | – | 6.00 | Bal. |
| **Max (wt.%)** | 0.15 | 2.00 | 2.00 | 0.045 | 0.015 | 19.00 | 0.80 | 0.110 | 9.50 | Bal. |

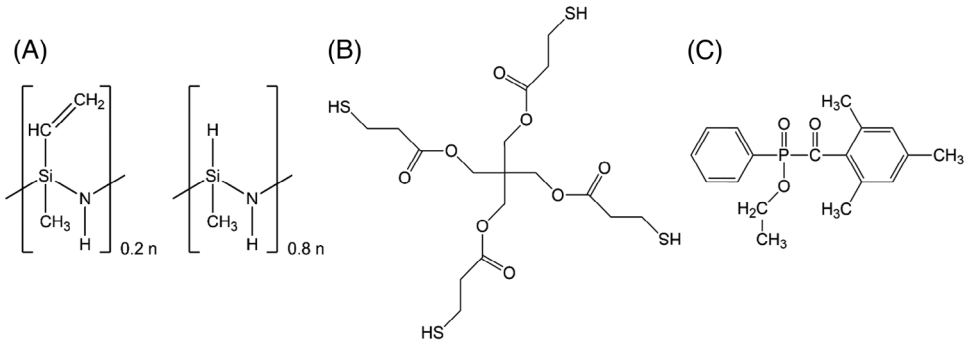


**FIGURE 1** Simplified chemical structures of the (A) organosilazane Durazane 1800, (B) crosslinking agent TT, and (C) photoinitiator TPO-L.

investigate the effect of the amount of the thiol crosslinker on the properties of the UV-crosslinked coatings. In addition, a photoinitiator (Ethyl (2,4,6-trimethylbenzoyl) phenylphosphinate, TPO-L, Figure 1C, Rahn AG, Switzerland) was added at a concentration of 5 wt.% based on the mass of precursor according to the work of Hoffmann et al.[34] Zinc flake pigments (Pro FLAKE Zn 1400, ECKART GmbH, Germany), zinc-magnesium flakes (STAPA® 15 ZnMg26, ECKART GmbH, Germany) and aluminum flakes (APS 11 micron, Alfa Aesar GmbH & Co. KG, Germany) were chosen as active corrosion protection fillers. After curing, the proportions of fillers were about 16 vol.% zinc flakes, 51 vol.% zinc-magnesium flakes and 13 vol.% aluminum flakes. This coating composition was investigated in a previous work and showed superior corrosion protection in saltwater corrosion tests.[37]

The preparation of the coating slurries started with dissolving the dispersing agent (DISPERBYK 2151, BYK-Chemie GmbH, Germany) in di-*n*-butylether (99+%, Acros Organics, Belgium), followed by the addition of the metallic fillers and stirring for 48 h. To avoid the premature activation of the photoinitiator by ambient UV light, the bottles were fully covered with an aluminum foil before TT and TPO-L were added to the systems intended for UV crosslinking. Hereafter, the precursor Durazane 1800 including DCP was added to the slurries for thermal curing while Durazane 1800 without DCP was added to the slurries for UV curing, respectively. The slurries were later applied onto both sides of the steel substrates using a semi-automatic spraying device equipped with a spray nozzle (model 780S, Nordson EFD, USA). For all samples, the same set of spraying parameters was used.

The crosslinking step of the thermally cured samples was carried out in a chamber furnace (LE 14/11, Nabertherm GmbH, Germany) at 250°C for 1 h in air with a heating rate of 3 K/min. This treatment led to a sufficient crosslinking of the silazane[38,39] and avoided thermal stressing of the substrate material.

Exposure of the filled UV-curable coating systems was conducted using high-power LEDs with a wavelength of 365 nm. The coated substrates were irradiated on both sides for two passes each via the UV conveyor belt (ConVey LED, Dr. Hönle AG, Germany) with a 100 HP IC 365 LED spot under ambient conditions. The intensity at the samples surface was 500 mW/cm$^2$ and the belt speed 0.1 m/min. In the following, the systems are referred to as "Thermally cured" corresponding to the thermally crosslinked coating system containing DCP while "10%", "50%", and "100%" according to the used amount of TT described above correspond to the UV-cured systems containing TT and TPO-L.

The microstructure of the coatings was characterized with a scanning electron microscope (SEM, Gemini Sigma 300VP, Carl Zeiss AG, Germany) with an acceleration

voltage of 10 keV and a working distance of 8.5 mm. The porosity of the coating systems was determined from several backscattered SEM images employing the software ImageJ and a Trainable Weka Segmentation tool.

To gain information about the surface roughness, the arithmetic mean roughness value $R_a$ and the averaged roughness depth $R_z$ were determined with a roughness measuring instrument (MarSurf PS 10, Mahr GmbH, Germany) according to the standard DIN EN ISO 4287. Microhardness tests were performed with a microhardness tester (Fischerscope HM2000, Helmut Fischer GmbH, Germany) to investigate mechanical properties of the coatings. Indentations were conducted using a Vickers indenter in the cross-sectional area applying a force of 50 mN. The loading and unloading time as well as the dwell time of the trapezoidal load function were set to 15 s and 5 s, respectively. Additionally, the scratch resistance was characterized using a scratch hardness tester (Lineartester Model 249, ERICHSEN GmbH & Co. KG, Germany) with a moving stylus according to the standard DIN ISO 1518 (Ø 1 mm, scratch speed 35 mm/s) at constant loads. The scratches were examined with a digital microscope (DSX 1000, EVIDENT Europe GmbH, Germany).

The chemical resistance to toluene (99.85%, ExtraDry, Acros Organics BVBA, Belgium) and isopropanol (Carl Roth GmbH + Co. KG, Germany) was determined by immersing coated samples for 24 h at room temperature. Toluene and isopropanol represented non-polar and polar media. Before and after the tests the thickness was measured with a micrometer screw and the contact angle of the coatings to water was analyzed before and after the immersion tests with a contact angle measuring device (DSA 25E, KRÜSS GmbH, Germany). The contact angle was measured approximately 5 s after the drop was applied onto the surface of the samples.

In order to analyze the curing mechanism, both the reactants and the coating system were examined by UV-Vis measurements. The measurements were conducted with a modular set up consisting of a light source (AvaLight-DH-S-BAL) and two detectors (AvaSpec-2048-2 and AvaSpec-UV/Vis/NIR, all Avantes B.V., The Netherlands). The results were evaluated using the software AvaSoft 7. For these measurements the coatings were applied on quartz glass substrates with a thickness of 2 mm and referenced to a WS-2 reference tile (Avantes B.V., The Netherlands), which is a PTFE-based standard for diffuse reflection. Analyses of the liquid precursor and the photoinitiator (Durazane 1800 and TPO-L) as well as a solution consisting of Durazane 1800, TT, TPO-L, and di-*n*-buthylether were performed in polystyrene and quartz glass cuvettes, respectively.

All tests and experiments were performed at room temperature in air.

**TABLE 3** Roughness values of UV-cured and thermally cured coatings on 1.7335 steel.

| System | 10% | 50% | 100% | Thermally cured |
|---|---|---|---|---|
| $R_a$ (µm) | 0.85 ± 0.08 | 0.94 ± 0.04 | 1.04 ± 0.06 | 1.01 ± 0.03 |
| $R_z$ (µm) | 5.20 ± 0.58 | 5.62 ± 0.12 | 6.31 ± 0.38 | 6.10 ± 0.19 |

## 3 | RESULTS AND DISCUSSION

In this section, first both curing methods are compared in terms of the microstructure, mechanical properties, and chemical resistance of the resulting coatings. Then the surface properties are examined by contact angle measurements and finally the curing mechanism of the UV-cured coatings is investigated.

### 3.1 | Microstructure of the coating systems

The microstructure of the coating systems after spraying was analyzed by SEM. Figure 2 shows cross-sectional images of the UV-cured coatings (10%, 50%, and 100%) and the thermally cured coating.

The thickness of the UV-cured coatings was in the range of 18–22 µm. The thickness of the thermally cured coating was similar with about 22 µm. In all coatings the metallic fillers were homogeneously distributed in the polysilazane matrix and aligned parallel to the substrate. The coatings possessed a porous microstructure caused by the high filler content of 80 vol.%. The porosity of the UV-cured coating systems ranged from 30% to 33%, which was again similar to the thermally cured one with about 31%.[37] The surface roughness values of the coatings are presented in Table 3. All values were in the same range, so eventually no significant differences in the microstructure and the surface roughness were determined.

### 3.2 | Mechanical characterization of the coating systems

Microhardness measurements and scratch resistance tests were carried out to compare the effects of both crosslinking processes on the mechanical properties. The results of the microhardness measurements are shown in Figure 3.

The mean hardness values of the UV-cured coatings including their standard deviation were 132 ± 10 MPa, 222 ± 17 MPa, and 255 ± 35 MPa for the 10%, 50%, and 100% samples, respectively. Therefore, the hardness of the UV-cured samples increased with a higher TT content. As

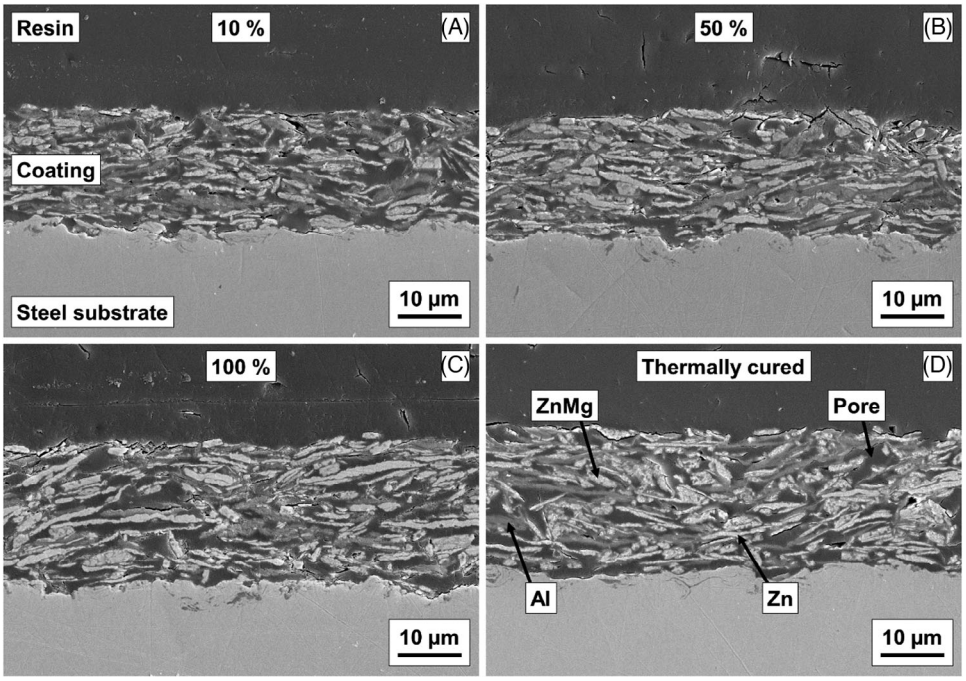


**FIGURE 2** SEM cross-sectional images of UV-cured and thermally cured coatings on 1.7335 steel: (A) 10%, (B) 50%, (C) 100%, and (D) thermally cured. The percentages refer to the molar ratio of thiol groups of the photoinitiator to vinyl groups of the precursor.

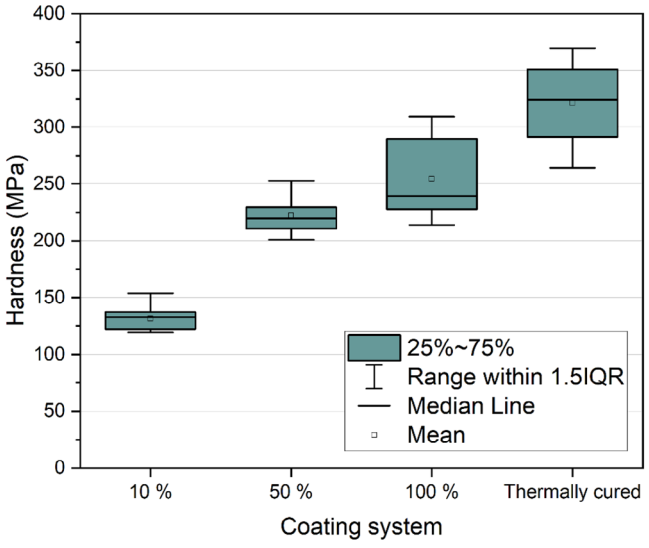


**FIGURE 3** Microhardness of UV-cured and thermally cured coatings on the 1.7335 steel substrate.

the TT content increases, more SH groups are available for crosslinking the precursor resulting in a more densely branched polymer network and thus higher hardness values. The mean hardness with standard deviation of the thermally cured coating system was 321 ± 32 MPa. Hence, by thermal curing a slightly higher hardness was achieved compared to UV curing method. Nevertheless, in general the measured values were relatively low due to the polymeric state of the silazane and the softness of the fillers themselves.

Images after performing scratch resistance tests at loads of 2–5 N are presented in Figure 4. At low loads of 2–3 N, the substrate was visible on all UV-crosslinked coatings and at 4 N large parts of the substrate were exposed. The scribe width remained the same for all UV-cured systems with about 300 µm, regardless of the force applied implying a plastic deformation behavior with very low resistance against penetration. In polymers that are crosslinked via the thiol-ene "click" reaction, flexible thioether bonds are incorporated within the network structure. These can reduce the overall mechanical properties and lead to plastic deformability of the material.[40,41] In case of the thermally cured coating, a scribe mark was also visible at a force of 2 N, but the substrate was not exposed. However, the scribe mark became wider at a higher force, which implies a deeper penetration depth of the stylus. From a load of 5 N, parts of the substrate were exposed and the scratch edges became rough indicating a slightly more brittle behavior that was not observed with the UV-cured coatings.

Even so, the failure at those loads can mainly be attributed to the porosity of the coatings, which reduces the mechanical properties and makes the coatings susceptible to scratches. These results are consistent with the conclusion from the microhardness measurement confirming slight differences in the mechanical properties as function of the curing method.

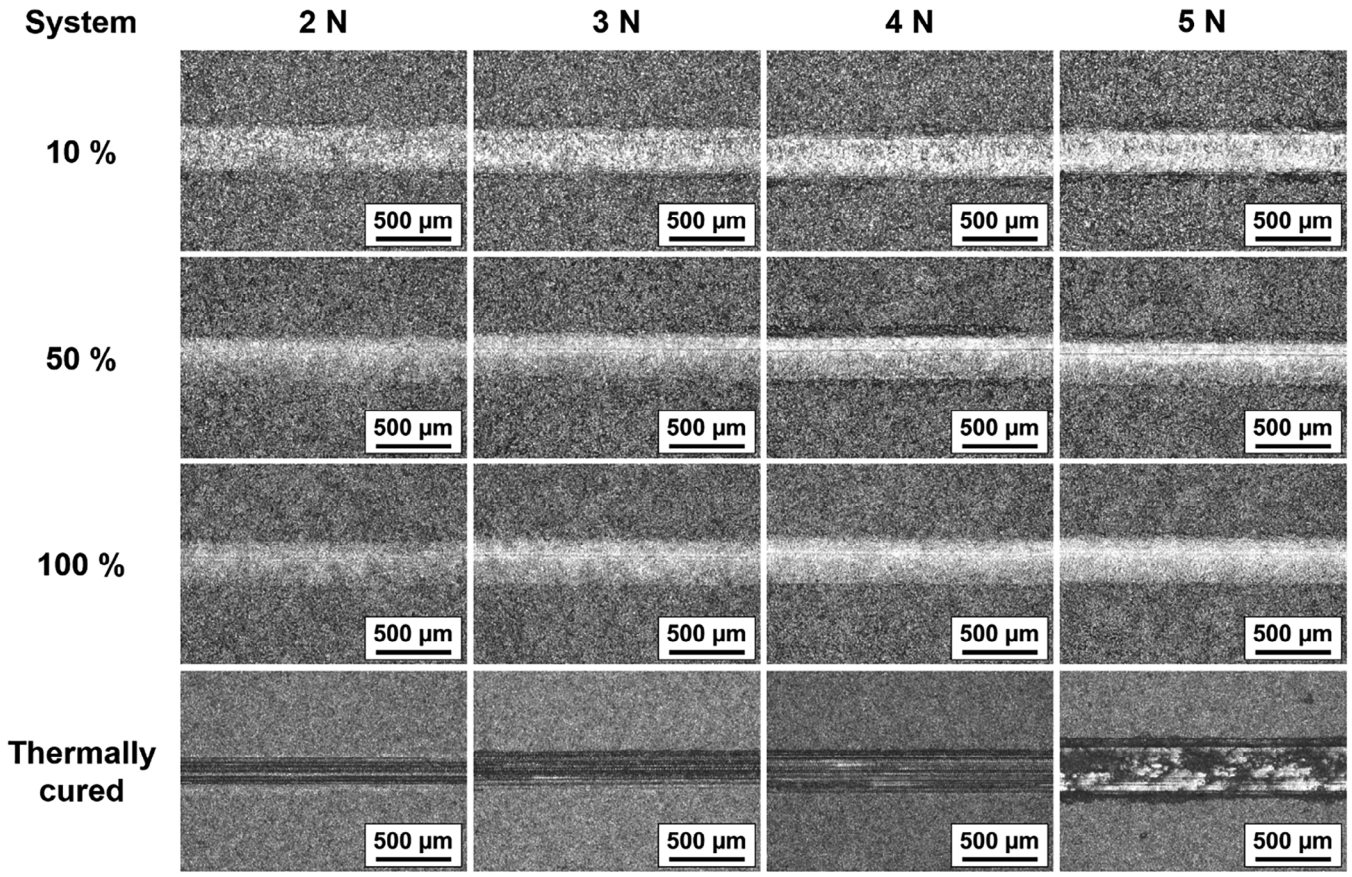


**FIGURE 4** Digital microscopy images of scratches on UV-cured and thermally cured coatings on steel 1.7335.

### 3.3 | Chemical resistance of the coating systems

As mentioned in the introduction, it was not clear whether the entire coating can be cured by UV irradiation. Chemical resistance tests in toluene and isopropanol were therefore carried out. For this purpose, the 10%, 100%, and thermally cured systems were selected. Samples were prepared on steel 1.4310, immersed in both chemical media at room temperature and removed after 24 h. Besides the visual appearance (Figure 5), the chemical resistance was evaluated by the change in coating thickness (Figure 6) and mass (Figure 7).

Figure 5 shows the surfaces of the coating samples after completing the tests in the respective media. The right side of each sample distinguished by the dashed lines was immersed.

After the tests in toluene and isopropanol, none of the coatings showed any change in optical appearance. Neither surface defects nor signs of detachment were visible. Even so, Hoffmann et al.[34] investigated the chemical resistance of unfilled polysilazane coatings, which were also crosslinked via the thiol-ene "click" reaction at room temperature, to various common solvents. After 24 h in water and isopropanol, they observed a slight optical clouding and streaking.

The measured changes in thickness of the coating systems during the chemical tests in both media and the area-related mass change of the samples are given in Figures 6 and 7, respectively.

After testing in toluene and isopropanol (Figure 6), a slight increase of coating thickness was measured for the 10% system while no significant deviation from the initial coating thicknesses were detected for the 100% and the thermally cured systems. This indicated a good resistance of the coatings to non-polar and polar solvents. Especially the good resistance to toluene demonstrated a full crosslinking of all systems because toluene is a common solvent for the Durazane 1800 precursor.[16,36] An inadequate crosslinking would have resulted in a dissolution of the coating matrix. As shown in Figure 7, very little to no mass loss occurred during the tests. To validate this result and to disclose spontaneous crosslinking, a reference sample with the same composition and preparation procedure as the UV-cured samples, which was not exposed to UV irradiation, was also tested in toluene. After less than 4 h

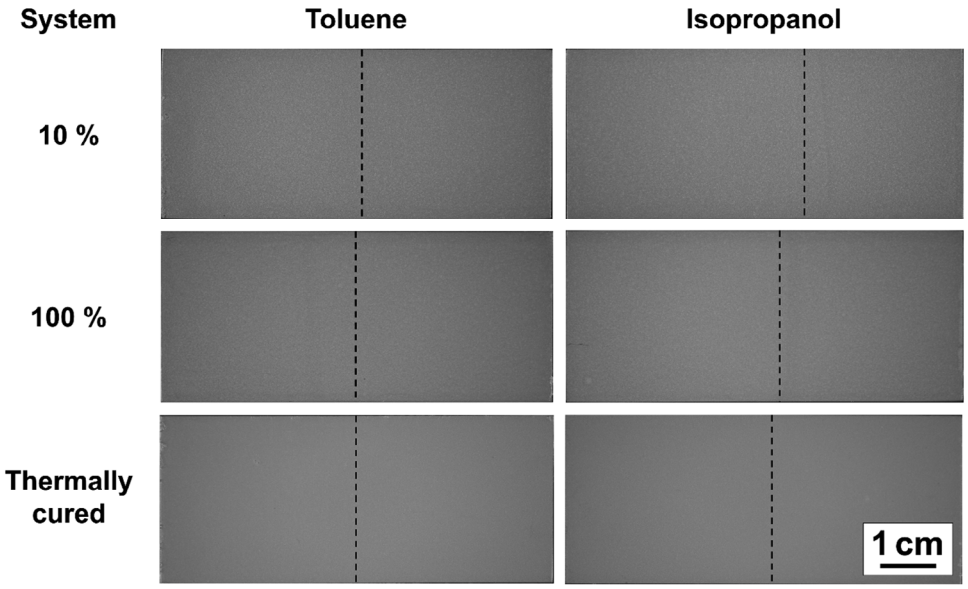


**FIGURE 5** Appearance of the UV-cured and thermally cured coatings on 1.4310 steel after immersion in toluene and isopropanol for 24 h at room temperature.

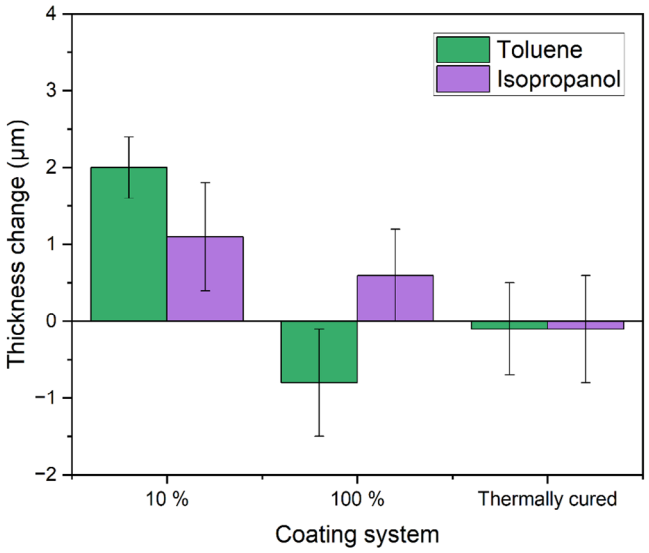


**FIGURE 6** Change of coating thickness of UV-cured and thermally cured coatings on 1.4310 steel after the immersion in toluene and isopropanol for 24 h at room temperature.

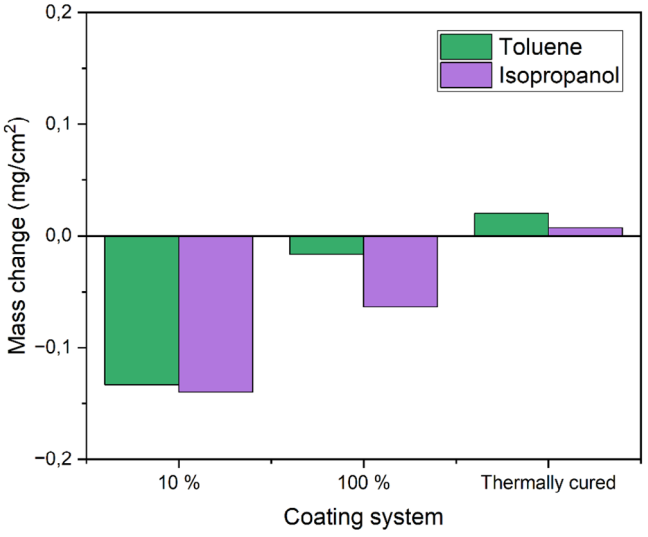


**FIGURE 7** Mass change of UV-cured and thermally cured coatings on 1.4310 steel during immersion tests in toluene and isopropanol for 24 h at room temperature.

the entire coating was detached from the substrate. Hence, the UV irradiation step clearly causes the good resistivity against toluene.

## 3.4 | Contact angle to water

Contact angle measurements with water were carried out to evaluate the changes in surface properties of the coating systems before and after the chemical resistance tests. Table 4 summarizes the contact angle values and Figure 8 depicts the contact angles of the samples before the chemical resistance tests.

As visible in Figure 8A and b and Table 4, both UV-cured coating systems showed contact angles of about 124°, while the thermally cured system had a lower contact angle of about 97°. Thus, the UV-cured coatings were significantly more hydrophobic, which could be beneficial for corrosion protection. Moreover, in case of the thermally cured system, the droplet was imbibed into the coating with increasing dwell time, which can be attributed to capillary forces due to the porosity. In general, the contact angle

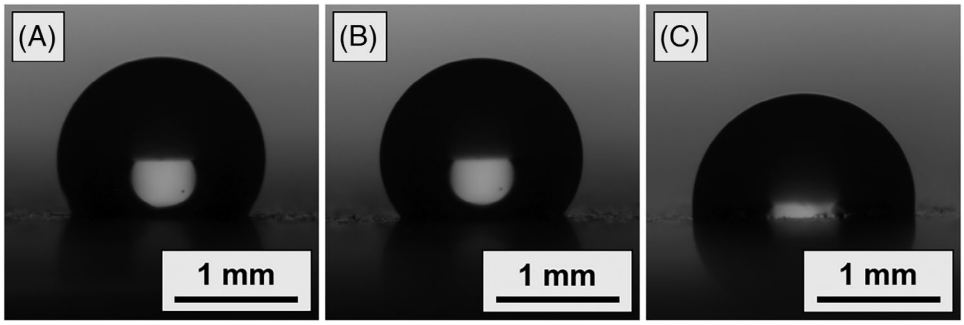


**FIGURE 8** Contact angle measurements with water on UV-cured and thermally cured coatings in air before the chemical resistance tests: (A) 10%, (B) 100%, and (C) thermally cured.

**TABLE 4** Contact angles to water of UV-cured and thermally cured coatings on steel 1.4310 before and after immersion in toluene and isopropanol for 24 h at room temperature.

| Coating system | Before immersion | After immersion in | |
|---|---|---|---|
| | | toluene | isopropanol |
| 10% | 124° ± 2° | 123° ± 1° | 123° ± 2° |
| 100% | 124° ± 3° | 126 ± 1° | 123° ± 2° |
| Thermally cured | 97° | 97° | 95° |

is mainly influenced by the structure of the surface and the surface energy.[42–46] Therefore, the difference between the behavior of the UV-cured and the thermally cured coating systems could arise due to a change of the chemical groups on the surface by oxidation during thermal treatment resulting in a change of surface polarity.

To get a deeper insight into the underlying mechanisms, additional measurements were carried out. For this purpose, a sample with the composition of the thermally cured coating system was applied on steel 1.4310 and dried in an oxygen-free atmosphere at room temperature. The aim of the following contact angle measurement was to exclude changes of the chemical properties of the surface due to reactions with oxygen during the thermal treatment at 250°C. The determined contact angle after drying was 127° ± 1° and the droplet was not imbibed. After the treatment at 250°C for 1 h in nitrogen atmosphere, the contact angle decreased only slightly to 119° ± 1°. Therefore, the behavior was comparable to that of the UV-crosslinked systems with approximately 124°. This test demonstrated that oxidation happens during thermal treatment at 250°C in air resulting in a change of the surface energy of the coatings. During thermal curing, the metallic fillers oxidize,[47–50] a conversion of Si-H groups and Si-N bonds of the silazane into the more hydrophilic Si-O-Si networks occurs,[39,51] and formed groups like Si-OH increase the polarity of the surface[51] thus determining the wetting behavior.[38] This led to a reduced contact angle of 97° after the thermal curing step in air.

Furthermore, in order to gain a better understanding of the role of the fillers, an unfilled UV-cured coating based on partially polymerized Durazane 1800 (HTTS)[34,52] without the metallic particles was prepared. For this purpose, a solution of 20 wt.% of HTTS in dimethylformamide (Carl Roth GmbH, Germany) with a TT content of 100% relative to the available vinyl groups and 5 wt.% of TPO-L relative to the mass of the used precursor was prepared. The solution was dip-coated on steel 1.4310 with a hoisting speed of 0.3 m/min and an immersion time of 10 s, followed by the same UV curing process as described above. This unfilled coating with a $R_a$ value of 0.13 ± 0.02 µm and a $R_z$ value of 0.85 ± 0.11 µm was considerably smoother than the filled coatings (Table 3) and revealed a contact angle of only 93° ± 2° to water. The hydrophobic character mainly resulted from hydrophobic organic groups such as Si−$CH_3$.[53] A similar HTTS-based and UV-cured coating on brushed stainless steel was investigated by Hoffmann et al.[34] yielding a similar contact angle of about 96°. Furtat et al.[54] determined the contact angle of a thermally at 130°C cured HTTS coating on stainless steel at about 97°. Hence, both results are in accordance with our value. This additional experiment revealed that the filler particles were responsible for an increase of the contact angle to about 124° compared to an unfilled UV-cured silazane-based coating by changing the morphology from a dense and flat to a porous and rough surface.

The contact angle values after the immersion tests in different liquids are summarized in Table 4. It is obvious that the contact angles of all coating systems did not change significantly during the tests in toluene and isopropanol, which is also a proof for the complete crosslinking of the UV-cured coatings.

## 3.5 | Investigation of curing mechanisms

As verified in the chemical resistance tests, the coatings were completely cured by UV-induced radical crosslinking

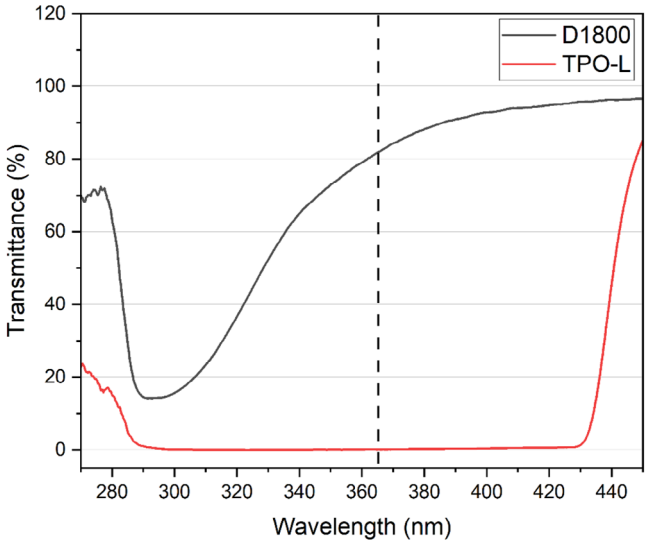


**FIGURE 9** UV-Vis transmittance spectra of pure organosilazane Durazane 1800 and pure photoinitiator TPO-L. Both measurements were conducted in a polystyrene cuvette.

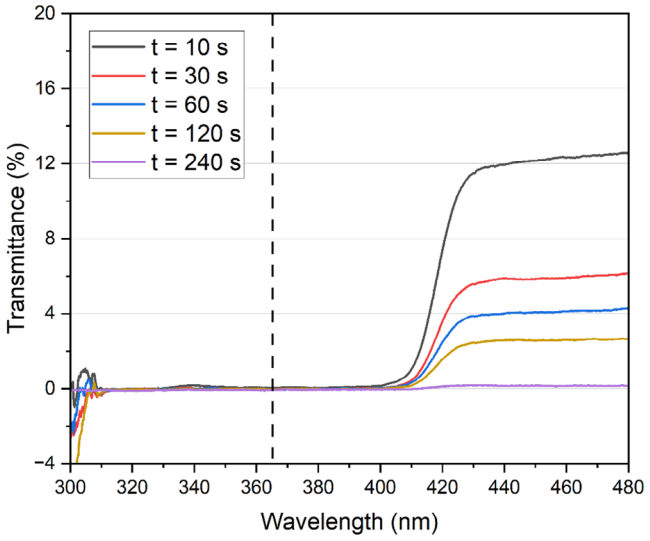


**FIGURE 10** UV-Vis transmittance spectra of a solution consisting of organosilazane Durazane 1800, photoinitiator TPO-L, and crosslinking agent TT in di-n-butylether according to the composition of the 100% system at selected time points after beginning of transmittance measurement.

reaction although the metallic filler particles are not UV transparent. To understand the crosslinking mechanisms of particle-filled coatings UV-Vis measurements were conducted. Initially, the transmittance of the organosilazane Durazane 1800 and the photoinitiator TPO-L was investigated (Figure 9). Afterward, a solution of the main components involved in the crosslinking reactions (Durazane 1800, TT, and TPO-L) in di-*n*-buthylether was measured (Figure 10). The solution was prepared according to the

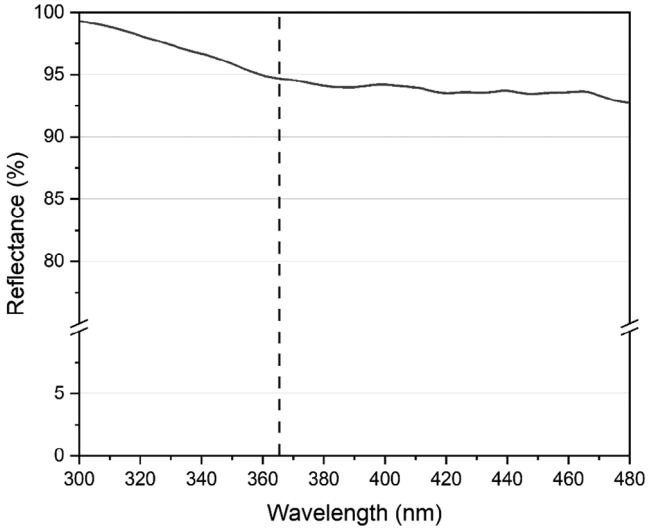


**FIGURE 11** UV-Vis reflectance of the 100% coating system on quartz glass using PTFE-based WS-2 standard as reference.

composition of the 100% system and investigated in a quartz glass cuvette using di-*n*-buthylether as reference. The transmittance of the solution was recorded over a period of several minutes to examine the changes of the spectrum with increasing irradiation time. Spectra of selected time points are depicted in Figure 10.

Durazane 1800 showed a high transmittance in the UV region with a value of about 81% at the curing wavelength of 365 nm (Figure 9). In contrast, TPO-L possessed no transmission in the UV region from 300 to 430 nm due to very strong absorbance of radiation within this range. Similarly, the solution of Durazane 1800, TT, and TPO-L did not exhibit any transmission in the range from 310 to 410 nm (Figure 10) for the same reason. However, a certain transmission at higher wavelengths (> 420 nm) was detected showing a decreasing trend with increasing measurement time as illustrated by the depicted spectra. This decrease in transmission can be attributed to ongoing crosslinking reactions initiated by the absorption of the low-intensity UV light of the instruments lamp. The incident light is scattered at crosslinked polysilazane structures leading to reduced transmittance. These results demonstrated the high sensitivity and effectivity of the thiol-ene "click" crosslinking reaction.

For the investigation of the coating system, the 100% system without any UV treatment applied on a quartz glass substrate was used. Since the metallic flakes reflect UV light, both the reflectance and the transmittance spectra of the coating system were measured simultaneously. As expected, a high reflection of about 95% (Figure 11) was observed, which can be ascribed to the presence of the metallic fillers, while the transmission was a flat line at 0% in the entire evaluated wavelength range within the

sensitivity of the detector (not shown). Therefore, only about 5% of the radiation at 365 nm was absorbed by the coating, mainly by the photoinitiator TPO-L (Figure 9).

Despite the low absorption, the particle-filled coating system was fully cured as demonstrated before. Therefore, crosslinking of the entire coating cannot occur only from direct UV irradiation at 365 nm alone as no radiation reached the backside of the coating.

Hence, we propose that curing could be supported by reflection and scattering of UV radiation at metallic filler particles, which are not perfectly oriented parallel to the substrate, acting as mirrors into deeper regions of the coating. This could be facilitated also by the porosity of the coatings. Additionally, only a small dose of radiation is needed to initiate the crosslinking reaction (Figure 10) as TPO-L has a very strong absorbance and the thiol-ene "click" reaction is highly effective. Furthermore, the radical reaction can also crosslink surrounding regions via radical propagation.

## 4 | CONCLUSION

In the present study, UV curing of a highly filled corrosion protection coating composed of a silazane matrix and metallic fillers was investigated for the first time. TT and TPO-L were chosen as reactants for the UV initiated thiol-ene "click" crosslinking reaction. The UV-cured coatings were compared to thermally cured ones (cured at 250°C for 1 h) regarding their microstructure, mechanical properties and chemical resistance to toluene and isopropanol. Furthermore, the curing mechanism was investigated by UV-Vis measurements.

The feasibility of curing the coating system by UV radiation was demonstrated. The complete curing resulted in a high resistance to toluene showing neither mass loss nor reduction in coating thickness. As UV-Vis measurements revealed a high reflectance of 95% and a transmittance of 0% of the coating, curing was not caused by direct irradiation alone. Mirroring of the radiation in to deeper regions of the coating facilitated by the porous structure was proposed as one possible mechanism to support curing. Characterization of the hardness and scratch resistance revealed that the mechanical properties of the UV-cured coating systems increased with increasing TT content reaching a maximum value that was only slightly lower compared to thermal curing. However, the UV-cured coatings exhibited a significantly higher contact angle to water compared to the thermally cured system, which can be beneficial for the corrosion protection properties of the coating system. The difference can be attributed to a change of surface polarity due to incorporation of oxygen in the precursor network and oxidation of the metallic fillers during the thermal treatment in air.

Hence, UV curing is a suitable alternative to thermal curing for both filled and unfilled coating systems achieving comparable properties. It offers particular advantages if a treatment in a furnace is not feasible or if temperature-sensitive components are used.

## ACKNOWLEDGMENTS

The authors have nothing to report.

Open access funding enabled and organized by Projekt DEAL.

## CONFLICT OF INTEREST STATEMENT

The authors declare no conflict of interest.

## ORCID

*Jan-Felix Wendel* https://orcid.org/0000-0002-2959-4303
*Daniel Leykam* https://orcid.org/0009-0001-9011-0603
*Stefan Schafföner* https://orcid.org/0000-0002-6526-2496
*Günter Motz* https://orcid.org/0000-0002-8010-068X

## REFERENCES

1. Hou B, Li X, Ma X, Du C, Zhang D, Zheng M, et al. The cost of corrosion in China. npj Mater Degrad. 2017;1(1):. https://doi.org/10.1038/s41529-017-0005-2
2. Feldmann F, Mears LLE, Roth M, Valtiner M. Characterisation of the galvanic protection of zinc flake coating by spectroelectrochemistry and industrial testing. Mater Corros. 2023;74(8):1148–58. https://doi.org/10.1002/maco.202213719
3. Plagemann P, Weise J, Zockoll A. Zinc–magnesium-pigment rich coatings for corrosion protection of aluminum alloys. Prog Org Coat. 2013;76(4):616–25. https://doi.org/10.1016/j.porgcoat.2012.12.001
4. Shreyas P, Panda B, Vishwanatha AD. Embrittlement of hot-dip galvanized steel: a review. In: M. Satyanarayana Gupta, TVK Gupta, and N. Kishore Nath, editors. 3rd International Conference on "Advancements in Aeromechanical Materials for Manufacturing," vol. 020038. AIP Publishing; 2021.
5. Rehrl J. Wasserstoffversprödung in hochfesten, mikrolegierten Stählen [Dissertation]. München: Technische Universität München; 2014. 186 p.
6. Kalendová A. Effects of particle sizes and shapes of zinc metal on the properties of anticorrosive coatings. Prog Org Coat. 2003;46(4):324–32. https://doi.org/10.1016/S0300-9440(03)00022-5
7. Vilche JR, Bucharsky EC, Giudice CA. Application of EIS and SEM to evaluate the influence of pigment shape and content in ZRP formulations on the corrosion prevention of naval steel. Corros Sci. 2002;44(6):1287–309. https://doi.org/10.1016/S0010-938X(01)00144-5
8. Abreu CM, Izquierdo M, Keddam M, Novoa XR, Takenouti H. Electrochemical behaviour of zinc-rich epoxy paints in 3% NaCl

solution. Electrochim Acta. 1996;41(15):2405–15. https://doi.org/10.1016/0013-4686(96)00021-7

9. Hussain AK, Seetharamaiah N, Pichumani M, Chakra CS. Research progress in organic zinc rich primer coatings for cathodic protection of metals—a comprehensive review. Prog Org Coat. 2021;153:106040. https://doi.org/10.1016/j.porgcoat.2020.106040
10. Schaefer K, Miszczyk A. Improvement of electrochemical action of zinc-rich paints by addition of nanoparticulate zinc. Corros Sci. 2013;66:380–91. https://doi.org/10.1016/j.corsci.2012.10.004
11. Pereira D, Scantlebury JD, Ferreira MGS, Almeida ME. The application of electrochemical measurements to the study and behaviour of zinc-rich coatings. Corros Sci. 1990;30(11):1135–47. https://doi.org/10.1016/0010-938X(90)90061-9
12. Wang J, Qi Y, Zhao X, Zhang Z. Electrochemical investigation of corrosion behavior of epoxy modified silicate zinc-rich coatings in 3.5% NaCl solution. Coatings. 2020;10(5):444. https://doi.org/10.3390/coatings10050444
13. Chen W-B, Chen P, Chen HY, Wu J, Tsai W-T. Developement of Al-containing zinc-rich paints for corrosion resistance. Appl Surf Sci. 2002;187:154–64. https://doi.org/10.1016/S0169-4332(01)00985-0
14. Amouzou D, Fourdrinier L, Maseri F, Sporken R. Formation of me–O–Si covalent bonds at the interface between polysilazane and stainless steel. Appl Surf Sci. 2014;320:519–23. https://doi.org/10.1016/j.apsusc.2014.09.109
15. Günthner M, Kraus T, Dierdorf A, Decker D, Krenkel W, Motz G. Advanced coatings on the basis of Si(C)N precursors for protection of steel against oxidation. J Eur Ceram Soc. 2009;29(10):2061–68. https://doi.org/10.1016/j.jeurceramsoc.2008.11.013
16. Colombo P, Mera G, Riedel R, Sorarù GD. Polymer-derived ceramics: 40 years of research and innovation in advanced ceramics. J Am Ceram Soc. 2010;93(7):1805–37. https://doi.org/10.1111/j.1551-2916.2010.03876.x
17. Barroso G, Li Q, Bordia RK, Motz G. Polymeric and ceramic silicon-based coatings—a review. J Mater Chem A. 2019;7(5):1936–63. https://doi.org/10.1039/C8TA09054H
18. Chaudhary RP, Parameswaran C, Idrees M, Rasaki AS, Liu C, Chen Z, et al. Additive manufacturing of polymer-derived ceramics: materials, technologies, properties and potential applications. Prog Mater Sci. 2022;128:100969. https://doi.org/10.1016/j.pmatsci.2022.100969
19. Qazzazie-Hauser A, Honnef K, Hanemann T. Crosslinking behavior of UV-cured polyorganosilazane as polymer-derived ceramic precursor in ambient and nitrogen atmosphere. Polymers (Basel). 2021;13(15). https://doi.org/10.3390/polym13152424
20. Reddy SK, Cramer NB, Cross T, Raj R, Bowman CN. Polymer-derived ceramic materials from thiol-ene photopolymerizations. Chem Mater. 2003;15(22):4257–61. https://doi.org/10.1021/cm034291x
21. Huang K, Marzi AD, Franchin G, Colombo P. UV-assisted robotic arm freeforming of SiOC ceramics from a preceramic polymer. Addit Manuf. 2024;83:104051. https://doi.org/10.1016/j.addma.2024.104051
22. Marzi AD, Diener S, Campagnolo A, Meneghetti G, Katsikis N, Colombo P, et al. Ultra-lightweight silicon nitride truss-based structures fabricated via UV-assisted robot direct ink writing. Mater Des. 2024;244:113092. https://doi.org/10.1016/j.matdes.2024.113092
23. Wang X, Schmidt F, Hanaor D, Kamm PH, Li S, Gurlo A. Additive manufacturing of ceramics from preceramic polymers: a versatile stereolithographic approach assisted by thiol-ene click chemistry. Addit Manuf. 2019;27:80–90. https://doi.org/10.1016/j.addma.2019.02.012
24. Zanchetta E, Cattaldo M, Franchin G, Schwentenwein M, Homa J, Brusatin G, et al. Stereolithography of SiOC ceramic microcomponents. Adv Mater. 2016;28(2):370–76. https://doi.org/10.1002/adma.201503470
25. Eckel ZC, Zhou C, Martin JH, Jacobsen AJ, Carter WB, Schaedler TA. Additive manufacturing of polymer-derived ceramics. Science. 2016;351(6268):58–62. https://doi.org/10.1126/science.aad2688
26. Feng Y, Guo X, Elsayed H, Huang K, Franchin G, Motz G, et al. Enhanced electromagnetic microwave absorption properties of SiCN(Fe) ceramics produced by additive manufacturing via in-situ reaction of ferrocene. Ceram Int. 2023;49(15):25051–62. https://doi.org/10.1016/j.ceramint.2023.05.035
27. Martínez-Crespiera S, Ionescu E, Schlosser M, Flittner K, Mistura G, Riedel R, et al. Fabrication of silicon oxycarbide-based microcomponents via photolithographic and soft lithography approaches. Sens Actuators, A. 2011;169(1):242–9. https://doi.org/10.1016/j.sna.2011.04.041
28. Martínez-Crespiera S, Ionescu E, Kleebe H-J, Riedel R. Pressureless synthesis of fully dense and crack-free SiOC bulk ceramics via photo-crosslinking and pyrolysis of a polysiloxane. J Eur Ceram Soc. 2011;31(5):913–9. https://doi.org/10.1016/j.jeurceramsoc.2010.11.019
29. Pan Z, Wang D, Guo X, Li Y, Zhang Z, Xu C. High strength and microwave-absorbing polymer-derived SiCN honeycomb ceramic prepared by 3D printing. J Eur Ceram Soc. 2022;42(4):1322–31. https://doi.org/10.1016/j.jeurceramsoc.2021.12.003
30. Zocca A, Colombo P, Gomes CM, Günster J. Additive manufacturing of ceramics: issues, potentialities, and opportunities. J Am Ceram Soc. 2015;98(7):1983–2001. https://doi.org/10.1111/jace.13700
31. Mikl G, Obmann R, Schörpf S, Liska R, Konegger T. Pore morphology tailoring in polymer-derived ceramics generated through photopolymerization-assisted solidification templating. Adv Eng Mater. 2019;21(6):. https://doi.org/10.1002/adem.201900052
32. Obmann R, Schörpf S, Gorsche C, Liska R, Fey T, Konegger T. Porous polysilazane-derived ceramic structures generated through photopolymerization-assisted solidification templating. J Eur Ceram Soc. 2019;39(4):838–45. https://doi.org/10.1016/j.jeurceramsoc.2018.11.045
33. Liew L-A, Liu Y, Luo R, Cross T, An L, Bright VM, et al. Fabrication of SiCN MEMS by photopolymerization of pre-ceramic polymer. Sens Actuators, A. 2002;95:120–34. https://doi.org/10.1016/S0924-4247(01)00723-3
34. Hoffmann M, Zahedtalaban M, Denk J, Horcher A, Ruckdäschel H, Schafföner S, et al. Photoinduced thiol-ene "click" chemistry for resource-efficient curing of polysilazane-based coatings and its effects on coating property profile. Open Ceram. 2023;15:100384. https://doi.org/10.1016/j.oceram.2023.100384

35. Hoyle CE, Bowman CN. Thiol-ene click chemistry. Angew Chem Int Ed Engl. 2010;49(9):1540–73. https://doi.org/10.1002/anie.200903924
36. Awin EW, Günther TE, Loukrakpam R, Schafföner S, Roth C, Motz G. Synthesis and characterization of precursor derived TiN@Si–Al–C–N ceramic nanocomposites for oxygen reduction reaction. Int J Appl Ceram Technol. 2023;20(1):59–69. https://doi.org/10.1111/ijac.14234
37. Wendel J-F, Matthée N, Schafföner S, Motz G. Silazane-based zinc-filled coating system for corrosion protection of steel in humid and salt water containing environments. J Am Ceram Soc. 2025. https://doi.org/10.1111/jace.20634
38. Barroso G, Döring M, Horcher A, Kienzle A, Motz G. Polysilazane-based coatings with anti-adherent properties for easy release of plastics and composites from metal molds. Adv Materials Inter. 2020;7(10):. https://doi.org/10.1002/admi.201901952
39. Günthner M, Wang K, Bordia RK, Motz G. Conversion behaviour and resulting mechanical properties of polysilazane-based coatings. J Eur Ceram Soc. 2012;32(9):1883–92. https://doi.org/10.1016/j.jeurceramsoc.2011.09.005
40. Beigi S, Yeganeh H, Atai M. Evaluation of fracture toughness and mechanical properties of ternary thiol-ene-methacrylate systems as resin matrix for dental restorative composites. Dental Mater. 2013;29(7):777–87. https://doi.org/10.1016/j.dental.2013.04.015
41. Cramer NB, Couch CL, Schreck KM, Carioscia JA, Boulden JE, Stansbury JW, et al. Investigation of thiol-ene and thiol-ene-methacrylate based resins as dental restorative materials. Dental Mater. 2010;26(1):21–28. https://doi.org/10.1016/j.dental.2009.08.004
42. Drelich JW, Boinovich L, Chibowski E, Della Volpe C, Hołysz L, Marmur A, et al. Contact angles: history of over 200 years of open questions. Surf Innovations. 2020;8(1-2):3–27. https://doi.org/10.1680/jsuin.19.00007
43. Young T. An essay on the cohesion of fluids. Philos Trans Royal Society London. 1805;95:65–87.
44. Wenzel RN. Resistance of solid surfaces to wetting by water. Ind Eng Chem. 1936;28(8):988–94.
45. Cassie A, Baxter S. Wettability of porous surfaces. Trans Faraday Soc. 1944;40:546.
46. Gao L, McCarthy TJ. How Wenzel and Cassie were wrong. Langmuir. 2007;23(7):3762–65. https://doi.org/10.1021/la062634a
47. Hammer GE, Shemenski RM. The oxidation of zinc in air studied by XPS and AES. J Vac Sci Technol, A. 1983;1(2):1026–28. https://doi.org/10.1116/1.572331
48. Isah K, Ramalan A, Jolayemi B. Structural, morphological and optical characteristics of low temperature oxidized metallic zinc films. BJAST. 2016;16(6):1–9. https://doi.org/10.9734/BJAST/2016/26853
49. Fournier V, Marcus P, Olefjord I. Oxidation of magnesium. SIA. 2002;34(1):494–7. https://doi.org/10.1002/sia.1346
50. Marcus P, Hinnen C, Olefjord I. Determination of attenuation lengths of photoelectrons in aluminium and aluminium oxide by angle-dependent x-ray photoelectron spectroscopy. SIA. 1993;20(11):923–9. https://doi.org/10.1002/sia.740201108
51. Wang K, Günthner M, Motz G, Flinn BD, Bordia RK. Control of surface energy of silicon oxynitride films. Langmuir. 2013;29(9):2889–96. https://doi.org/10.1021/la304307y
52. Flores O, Schmalz T, Krenkel W, Heymann L, Motz G. Selective cross-linking of oligosilazanes to tailored meltable polysilazanes for the processing of ceramic SiCN fibres. J Mater Chem A. 2013;1(48):15406. https://doi.org/10.1039/c3ta13254d
53. Zhan Y, Grottenmüller R, Li W, Javaid F, Riedel R. Evaluation of mechanical properties and hydrophobicity of room-temperature, moisture-curable polysilazane coatings. J Appl Polym Sci. 2021;138(21). https://doi.org/10.1002/app.50469
54. Furtat P, Lenz-Leite M, Ionescu E, Machado RAF, Motz G. Synthesis of fluorine-modified polysilazanes via Si–H bond activation and their application as protective hydrophobic coatings. J Mater Chem A. 2017;5(48):25509–21. https://doi.org/10.1039/C7TA07687H


**How to cite this article:** Wendel J-F, Fischer A, Leykam D, Schafföner S, Motz G. UV curing of polysilazane-based coatings with metallic fillers for corrosion protection applications. Int J Appl Ceram Technol. 2025;22:e70034. https://doi.org/10.1111/ijac.70034